ELSEVIER

Journal of Nuclear Materials 302 (2002) 193–205

journal of nuclear materials

www.elsevier.com/locate/jnucmat

Systematic study of formation of soft and hard zones in the dissimilar weldments of Cr–Mo steels

C. Sudha [a], A.L.E. Terrance [a], S.K. Albert [b], M. Vijayalakshmi [a,*]

[a] *Physical Metallurgy Section, Materials Characterisation Group, Indira Gandhi Centre for Atomic Research, Kalpakkam 603 102, India*
[b] *Materials Joining Section, Materials Development Division, Indira Gandhi Centre for Atomic Research, Kalpakkam 603 102, India*

Received 23 October 2001; accepted 15 January 2002

Abstract

The microstructural stability and elemental redistribution in dissimilar weldments between 9Cr–1Mo and 2.25Cr–1Mo ferritic steels during various postweld heat treatments (PWHTs) have been studied using microscopy techniques ranging from optical to transmission electron microscopy and electron probe microanalyser. Application of PWHT at 1023 K for various times resulted in the formation of a soft zone in the low Cr side and a carbide rich hard zone adjoining the soft zone in the high Cr side of the weldment. The width of these zones and their hardness are influenced by the time of exposure at elevated temperature. A measurable increase in the width and a decrease in the hardness of the soft and hard zones with aging times are observed. Correlation between these observed effects and the elemental redistribution responsible for the formation of these zones is being attempted. Micromechanisms responsible for the formation of these zones are proposed. Migration of carbon from low Cr side to high Cr side driven by the gradient in the carbon activity has been found to be responsible for the formation of these zones. © 2002 Published by Elsevier Science B.V.

1. Introduction

Dissimilar steel joints are widely used in many components in chemical, petrochemical and nuclear industry. In the fabrication of steam generators for thermal or nuclear power plants, both high Cr and low Cr steels are employed [1], depending on the service temperature experienced by different parts of the steam generator such as super heater, preheater etc. This results in dissimilar welding in selected locations. Postweld heat treatment (PWHT) of dissimilar welds between Cr–Mo steels differing in Cr content or between a Cr–Mo steel and an austenitic stainless steel [2] often result in the formation of a carbon depleted soft zone in the low Cr side and a precipitate (mainly carbides) rich zone in the high Cr side. This is attributed [3] to the migration of carbon from low Cr side to high Cr side as a consequence of the difference in the activities of carbon of the two steels. Some of the studies discussed [4,5] the effect of carbon migration in Cr–Mo weldments on various mechanical properties. Computations to predict the width of carbon depleted soft zone in the low Cr side and carbide rich zone in high Cr side have also been carried out [6]. Even though attempts have been made [1,4] to determine the elemental redistribution (mainly of Cr and Mo) across the weld interface in dissimilar weldments between 9Cr–1Mo and 2.25Cr–1Mo steel, a systematic direct study of carbon redistribution has not been attempted so far which has been the primary aim of the present study.

In the present study, formation of soft and hard zones in the weldments of 9Cr–1Mo and 2.25Cr–1Mo steels subjected to PWHT at 1023 K are investigated in detail. Based on detailed microstructural studies different stages of formation of these zones are identified and micromechanisms responsible for these stages are proposed.

* Corresponding author. Tel.: +91-4114 80 306; fax: +91-4114 80 081/306/360.
E-mail address: mvl@igcar.ernet.in (M. Vijayalakshmi).

0022-3115/02/$ - see front matter © 2002 Published by Elsevier Science B.V.
PII: S0022-3115(02)00777-8

2. Experimental

Two ferritic steels, 2.25Cr–1Mo and 9Cr–1Mo in the normalised and tempered condition were used as base plates for the preparation of dissimilar weld pads, the composition of which are given in Table 1. Shielded metal arc welding process was employed in the preparation of dissimilar weld pads between 12 mm thick 2.25Cr–1Mo and 9Cr–1Mo steel plates using 9Cr–1Mo as electrode and the welding parameters are given in Table 2. The weld pads were given PWHT at 1023 K for different time durations like 1, 2, 5, 10 and 15 h. Microstructural examination was carried out using an optical microscope (Model no: MEF4A of M/s Leica). The weld pads were polished and etched using Vilella's reagent and 2% Nital solution for microstructural examination. Nital being a mild reagent etches only the 2.25Cr–1Mo side. Leitz Miniload2 microhardness tester was used for microhardness studies measured with a 200 g load. Width and hardness of the soft zone as well as the precipitated zone were measured. Scanning electron microscope (XL30 ESEM of M/s Phillips) was used to get high magnification secondary electron image of the precipitates in hard zone and the ferrite grains in soft zone. Cross-section of the weldment across which the study was carried out is shown in Fig. 1. The region of interest in the present study is confined to the interface between the 2.25Cr–1Mo base metal and 9Cr–1Mo weld metal and the plane of observation is along the middle section of the weld as shown by dotted lines in Fig. 1.

The concentration profiles of iron, chromium, molybdenum and carbon were carried out using a Cameca SX50 electron probe microanalyser (EPMA) to determine the elemental redistribution across the weld interface. Accelerating voltage of 20 kV was used for the analysis. Crystals used were LiF for FeKα and CrKα, PET for MoLα and PC2 for CKα. The diameter of the beam used was about 1 μm. Quantitative analysis was performed comparing the intensities of the Kα or Lα radiation of the elements obtained from the sample with that of the standard. A specialised computer package called as QUANTA was used for quantitative analysis, which takes care of the corrections to be made while calculating the concentrations of various elements. X-ray mapping for Cr and C was done across the interface between the hard and soft zones for a resolution of 256×256 pixels at a scanning speed of 100 ms per pixel.

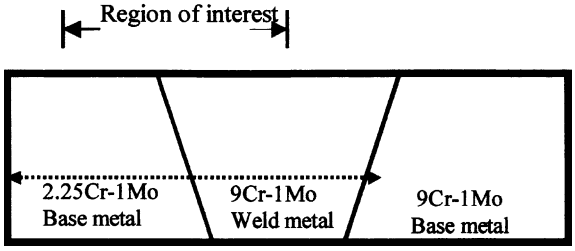

Fig. 1. Cross-section of the weldment under study (dotted lines indicate the plane of observation and arrow marks show the region of interest).

A Philips CM200 transmission electron microscope (TEM) was used to investigate the type and morphology of carbides present in the hard zone for 1023 K 15-h heat treated sample. Selected area diffraction (SAD) patterns obtained from the carbides on the extraction replicas were examined to identify the nature of carbides. Carbon extraction replicas, selectively from the hard zone of few μm thick, were prepared as follows: After etching the sample with 2% Nital solution, the hard zone alone was carbon coated by masking the remaining regions of the sample with thin aluminium foil. After carbon coating, the aluminium foil was removed, leaving a thin film of carbon along the hard zone of the sample. On

Table 1
Chemical composition of the steel plates and the weld metal

Serial no.	Description	Element (wt%)						
		C	Cr	Mo	Mn	S	P	Si
1	2.25Cr–1Mo plate	0.12	2.18	1.0	0.46	0.001	0.01	0.25
2	9Cr–1Mo plate	0.07	8.24	1.0	0.36	0.001	0.02	0.21
3	9Cr–1Mo weld metal (electrode)	0.08	10.25	0.98	0.91	0.02	0.02	0.40

Table 2
Welding parameters employed for preparation of weld pads

Electrode diameter (mm)	Preheat temperature (K)	Current (A)	Voltage (V)	Welding speed (mm/min)	Joint geometry	Bead tech	No. of layers
4	493	160–175	26	140	Single V	Stringer	8

etching the sample again with 2% Nital solution, the carbon film got detached from the sample. These films were collected on a 200-mesh grid and examined in TEM.

3. Results

The results are presented in the following sequence: the evidences for the formation of 'soft' and 'hard' zones when dissimilar weldments of 2.25Cr–1Mo and 9Cr–1Mo are exposed to elevated temperature are presented initially. The variation of the width and hardness of these zones is studied systematically in Section 3.1. Section 3.2 deals with the microchemical redistribution of the constituent elements leading to the formation of such zones, which is discussed based on EPMA results. Finally a direct confirmation for the presence of carbides in the hard zone is given based on TEM studies.

3.1. Formation of soft and hard zones in dissimilar welds

Fig. 2(a) shows the microstructure of the weldment on etching with 2% Nital solution. It is found that the 9Cr–1Mo weld metal side has not been etched by the reagent, while the 2.25Cr–1Mo base metal side showed a tempered bainitic structure. This is in agreement with the structure expected for normalised and tempered 2.25Cr–1Mo steel. On etching with Vilella's reagent the as welded, starting material was found to retain a martensitic structure on the 9Cr–1Mo weld metal and a tempered bainitic structure on the 2.25Cr–1Mo base metal side. On the fusion line it was observed that lightly etched bands commonly referred [1] as unmixed zones or intermediate mixed zones are present. Fig. 2(b) shows the microhardness profile across the as welded specimen. The hardness of the weld metal i.e. 9Cr–1Mo corresponding to the martensitic structure is above 400 VHN. Heat affected zone (HAZ) of the base metal has a hardness of around 360 VHN while the hardness in the 2.25Cr–1Mo base metal, 3 mm away from the fusion line is ~225 VHN.

Fig. 3(a) shows the microstructure of the weldment exposed to 1023 K for 15 h and the corresponding microhardness profile is shown in Fig. 3(b). On exposure of the weldment to 15 h of heat treatment, microstructural changes were observed on the weld metal side as well as in the region between the weld metal and the 2.25Cr–1Mo base metal. There is a heavily etched band on the weld metal side (marked as A in Fig. 3(a)), which is found to be precipitate rich and discontinuous in nature. Fig. 3(c) shows the high magnification secondary electron image of very fine precipitates present in this region. Hardness profile taken across the weld interface shows very high hardness (~271 VHN) on this region. Hence it may be called as the *hard zone* or *precipitate rich* band. Near the fusion boundary region on the HAZ a lightly etched band is seen (marked as B in Fig. 3(a)), which is continuous throughout the fusion line. Fig. 3(d) clearly shows the ferrite grains present in this zone. This lightly etched band may be called as the *soft zone*, since it is characterised by the lowest hardness (~120 VHN) and the absence of precipitates. Such bands have not been observed in as welded samples. Earlier studies carried out on dissimilar weldments, have reported [7–9] the formation of such hard and soft zones in the weld interface on subjecting the dissimilar weldments to PWHT.

Microstructures of the weldments heated to 1023 K for 1, 2 and 10 h are shown in Fig. 4(a)–(c). The formation and gradual growth of the width of soft zone

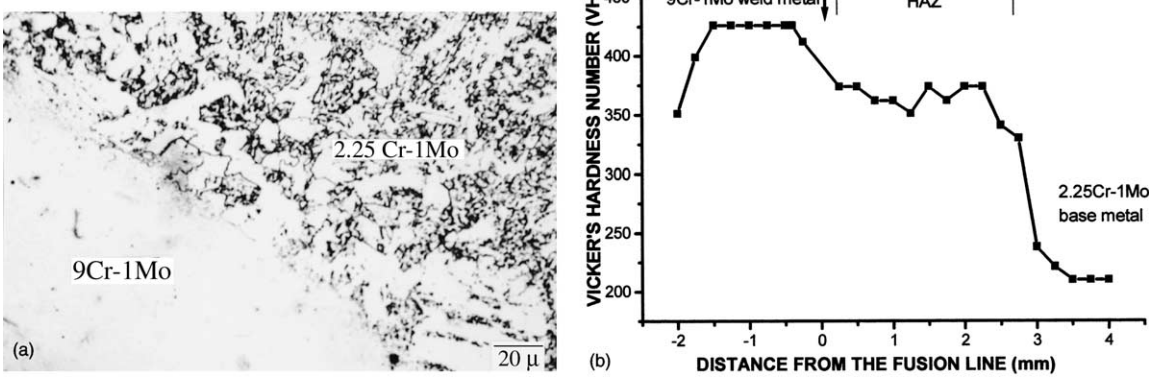

Fig. 2. (a) Optical micrographs of 'as welded' specimens etched with 2% Nital solution, (b) Vicker's microhardness profile of as welded specimen (load = 200 g).

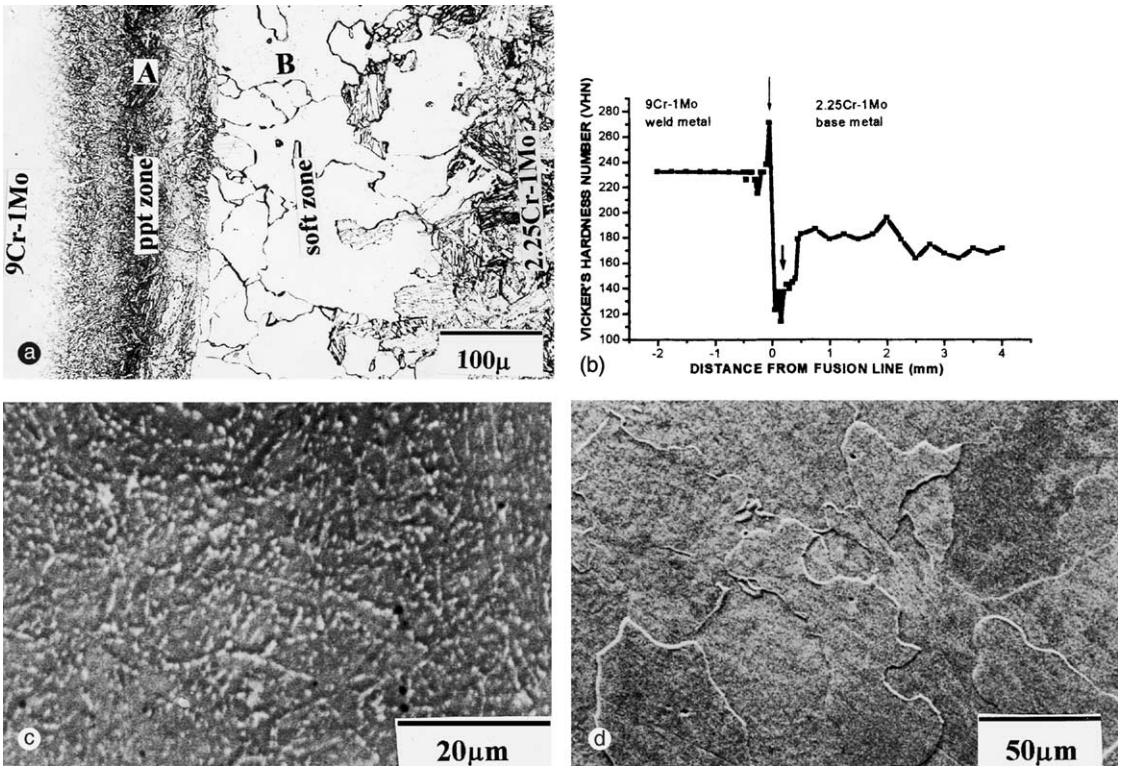

Fig. 3. (a) Optical micrograph of 15-h treated sample etched with 2% Nital solution showing hard and soft zones (A-hard zone and B-soft zone) (ppt-precipitate zone). Observe the differences between as welded (Fig. 2(a)) and heat treated specimen, (b) Microhardness profile across the fusion line showing increase in hardness for the hard zone (dotted arrows) and decrease in hardness for the soft zone (solid arrows). Note the absence of these variations in Fig. 2(b) for as welded sample, (c) SE image of precipitates in hard zone and (d) SE image of ferrite grains in soft zone, devoid of secondary phases.

and hard zone are clearly seen in the micrographs. It is observed that width of the soft zone as well as the precipitate rich band increases with time of heat treatment. Microstructural examination shows that widths of both bands are not uniform throughout the weld interface. Microhardness measurements for the samples taken across the weld interface are shown in Fig. 5. Hard and soft zones are found to appear within as short a time as 1-h heat treatment. As the time of heat treatment increases, hardness of the recrystallized zone and the precipitate rich band decreases. Variation of the average width of these zones and their hardness with the heat treatment times is shown in Fig. 6(a) and (b). It can be seen that width of the soft and hard zone increases with time till their rate of change slows down considerably for longer aging times. Fig. 6(b) shows that hardness of the soft zone decreases rapidly from ~185 to 125 VHN, after which there is no further decrease. Hardness of the precipitate rich band decreases only from ~280 to 265 VHN. Both the width as well as the hardness do not show any change after 10 h of heat treatment. Hence, it can be justifiably presumed that the transformation responsible for the changes in hardness slows down considerably after 15 h of heat treatment at 1023 K.

3.2. Elemental redistribution in the zones

The line scans performed for as welded and 15-h heat treated sample to determine the redistribution of Cr and C across the weld interface are shown in Fig. 7(a) and (b) respectively. Fig. 7(a) shows that the Cr concentration for both the as welded and the heat treated sample decreases rapidly across the interface, which is due to the difference in the chemical composition between the 9Cr–1Mo weld metal and 2.25Cr–1Mo base metal. From the plot of as welded specimen in Fig. 7(a) it is seen that dilution in the weld metal is limited to 0.1 mm. From Fig. 7(b) it is found that there is an increase in the carbon concentration for the heat treated sample on the weld metal side of the interface. A decrease in carbon concentration on the base metal side after heat treatment is also observed. No significant change in molybdenum concentration was observed. The line scan

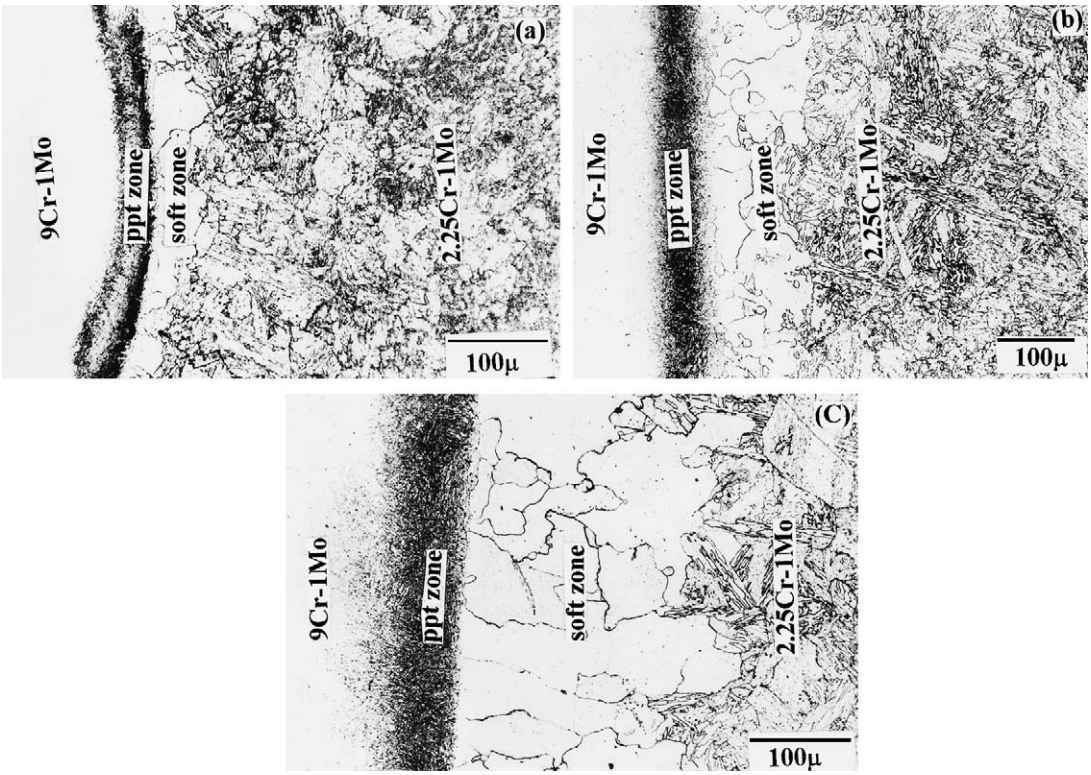

Fig. 4. Optical micrographs of dissimilar weldments aged at 1023 K for (a) 1, (b) 2 and (c) 10 h. A gradual increase in the width of the soft and hard zones is visible with increase in heat treatment times (ppt-precipitate zone).

obtained for the samples aged for various time durations of 1, 2, 5 and 10 h also showed a similar trend for Cr, Mo and C across the interface. In order to get a qualitative comparison of the difference in carbon and chromium in the hard and soft zones, X-ray emission spectrum in these regions were obtained using PC2 and PET crystals (Fig. 8(a)–(d)). It shows that the carbon concentration in the hard zone is quite high compared to that of soft zone. A distinct difference in the ratio of the concentrations of Cr and Fe was observed between the hard and soft zones. Change in the overall chromium concentration may be due to the nominal chemical composition. Quantitative analysis performed for the 15-h heat treated sample is shown in Fig. 9(a) and (b). Cr concentration (Fig. 9(a)) shows a decrease across the interface from the weld metal to the base metal, but a scatter in the profile is observed near the interface on the weld metal side. The molybdenum content was found to be uniform throughout the region of interest. A plot of the concentration profile for C (Fig. 9(b)) shows the enrichment of carbon on the precipitate rich band. An accurate quantitative analysis for carbon could not be performed since the standard used was pure diamond. It is known that it is not possible to detect the low percentages of carbon. X-ray images for carbon and chromium taken across the interface of the hard and soft zone is shown in Fig. 10(a) and (b) respectively. The grey scale increases from black (minimum detectable limit) to white (maximum detectable limit). Grey scale of black corresponds to the absence of the element (0%) and white indicates maximum enrichment of the element (100%) at a particular point. It shows the presence of high density of fine precipitates in the hard zone. A line scan was performed exclusively on the hard zone in an attempt to identify these precipitates and Fig. 11 shows the same. The enrichment of chromium and carbon at the same location (arrow marked) suggests the presence of Cr rich carbides.

3.3. Direct confirmation for the formation carbides in hard zone

All the above experiments, like high hardness and enrichment of chromium and carbon suggest the presence of chromium rich carbides in the hard zone. In order to obtain a direct evidence for the same, transmission electron microscopy was carried out on carbon extraction replicas prepared from the hard zone alone. Fig. 12(a) and (b) show two typical microstructure and SAD patterns for the precipitates present in hard zone.

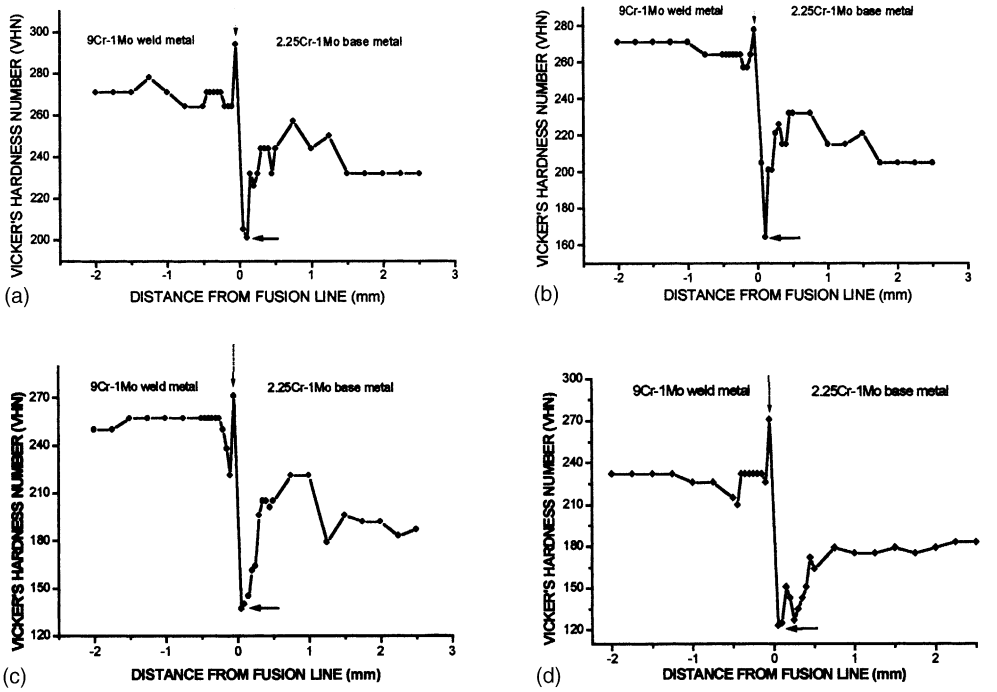

Fig. 5. Hardness profile for PWHT samples (a) 1, (b) 2, (c) 5 and (d) 10 h. A high hardness near the fusion line on 9Cr side corresponds to the hard zone (dotted arrows) and the low hardness near the fusion line on 2.25Cr side corresponds to soft zone (solid arrows). Decrease in hardness of both the zones with increase in time of heat treatment is evident.

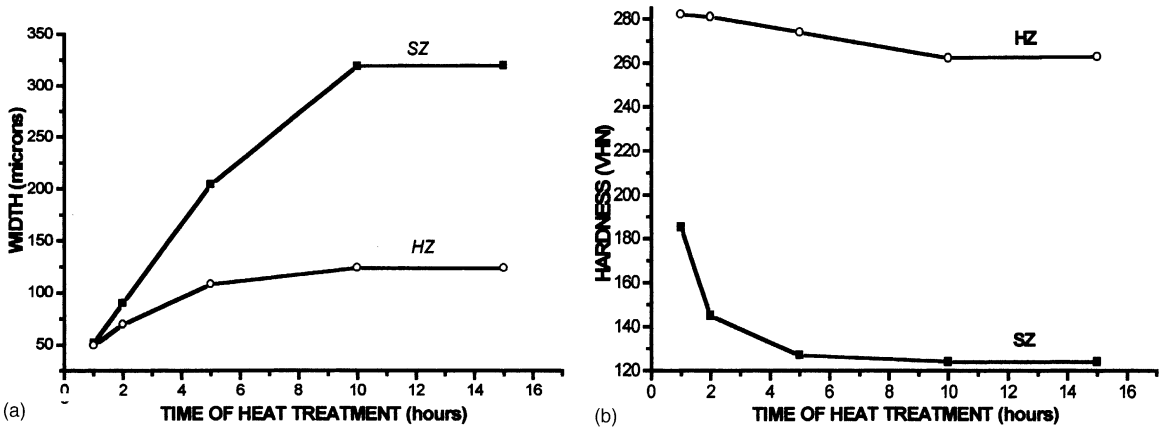

Fig. 6. Variation of (a) width and (b) Vicker's hardness (load = 200 g) with time of heat treatment (SZ: soft zone, HZ: hard zone). Rate of change in width and hardness reduce for longer heat treatment times.

The precipitates in the hard zone were found to be of different sizes and morphology. Most of them are found to be coarse, globular though some are fine and lenticular. Analysis of SAD patterns from both types of carbides confirmed these precipitates to be Cr rich $M_{23}C_6$ carbides. The different morphology of $M_{23}C_6$ carbides in the microstructures suggest that these carbides are probably at various stages of their growth.

3.4. Summary of experimental results

The results presented above may be summarised as follows:

- PWHT of dissimilar weldments between 2.25Cr–1Mo and 9Cr–1Mo ferritic steels result in the formation of hard and soft zones.

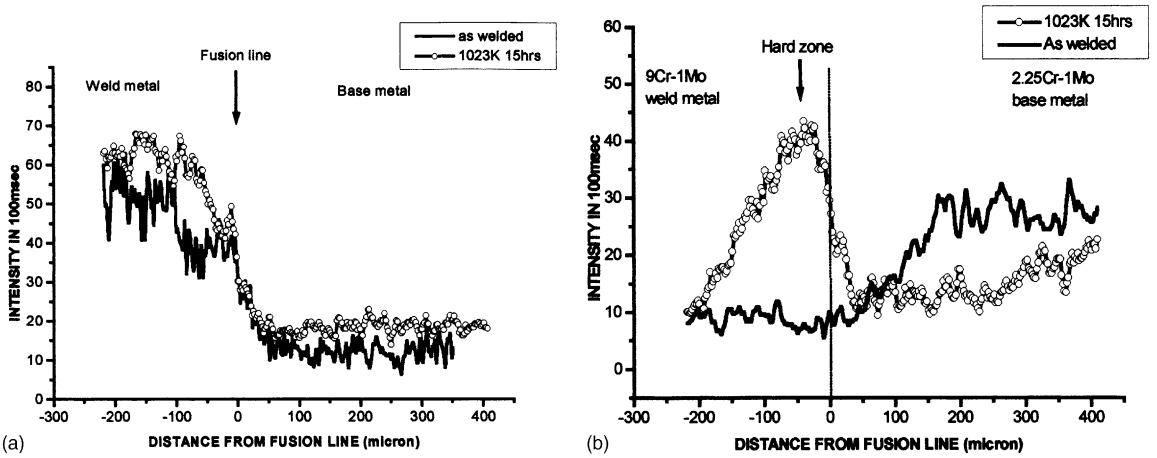

Fig. 7. Concentration profile across the weld interface for (a) Cr and (b) C for 1023 K 15-h heat treated sample. The increase in Cr across the interface may be due to the inherent difference in chemical composition of the two constituent base metals, 9Cr and 2.25%Cr. Note the substantial increase in carbon content near the interface on 9Cr side corresponding to hard zone.

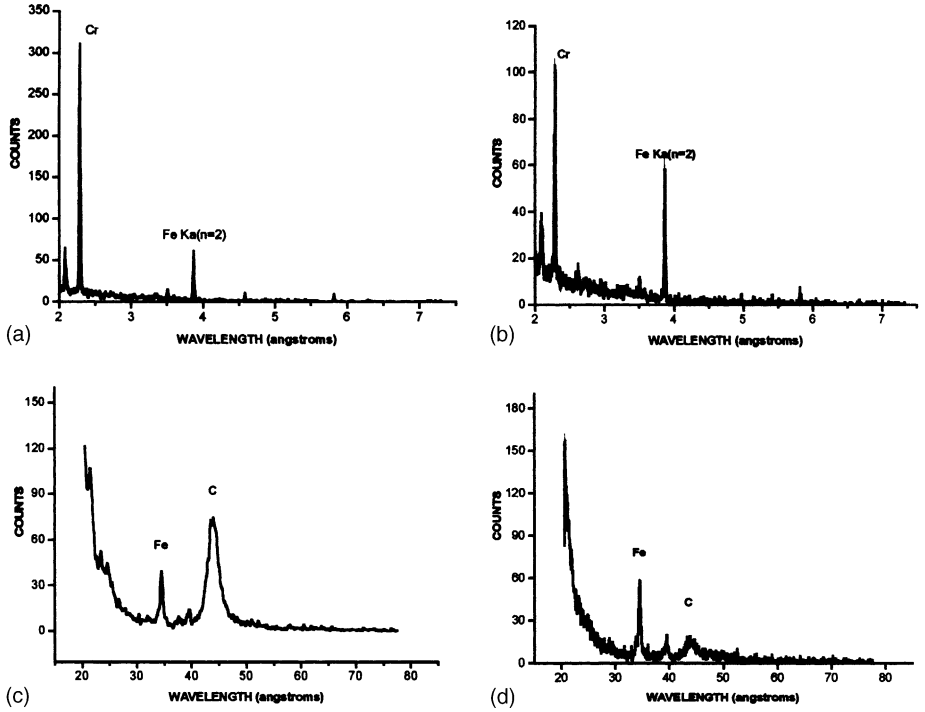

Fig. 8. Confirmed evidence for the enrichment of C in hard zone. Comparative X-ray spectrum for Cr in (a) hard zone, (b) soft zone taken using PET crystal and for C in (c) hard zone and (d) soft zone taken using PC2 crystal for 1023 K 15-h heat treated sample.

- Width and hardness of these zones vary with the time of heat treatment.
- As the time of heat treatment increases, hardness of hard zone decreases and the width marginally increases. It is characterised by the presence of very fine precipitates.
- Soft zone, which is characterised by the absence of precipitates, shows a significant increase in width and a decrease in hardness with the time of heat treatment.
- Changes in width and hardness are found to slow down considerably for long aging times.

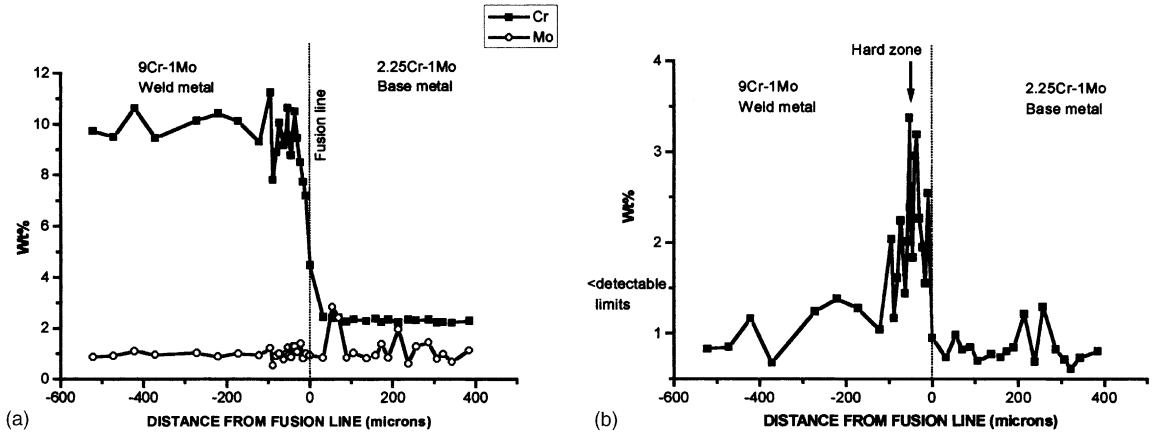

Fig. 9. Elemental concentration across the weld interface for (a) Cr and Mo and (b) C for 1023 K 15-h heat treated sample. Shows an increase in Cr content across the interface which may be only due to the difference in chemical composition between the base metal (2.25Cr–1Mo) and the weld metal (9Cr–1Mo).

- Microchemical characterisation showed that the carbon concentration is maximum at the precipitate rich zone and suggested that the carbides present in the hard zone may be chromium rich carbides.
- Transmission electron microscopy on carbon extraction replica from the hard zone confirmed the presence of chromium rich $M_{23}C_6$ carbides in the hard zone.

4. Discussion

The evidences presented in the previous section, regarding the changes in the microstructure, elemental redistribution and consequent changes in hardness of the dissimilar weldments on exposure to 1023 K will be discussed in the present section.

4.1. As-welded structure

The base metals, used in the present study, are the 2.25Cr–1Mo and 9Cr–1Mo steel, in the normalised and tempered state. The 2.25Cr steel is found to exhibit a tempered bainitic structure with hardness of around 225 VHN and the high Cr steel has a hardness of around 350 VHN, suggesting a martensitic structure, consistent with the initial treatment.

The microstructure and the hardness profile of as-welded sample can be understood in terms of the thermal cycle the base metals are subjected to, during the process of welding. Let us consider the low-chrome side first. It is expected the zone of 2.25Cr base metal close to the weld metal is heated beyond the Ac1 temperature (temperature at which ferrite changes to austenite) during the heating part of weld thermal cycle and thus enters the austenite phase field. Depending on the cooling rate the austenite can undergo a martensitic or bainitic transformation. The observation (Fig. 2(b)) of high hardness value of 375 VHN of the HAZ of 2.25Cr base metal and the microstructure (Fig. 2(a)) shows that for the present welding conditions the 2.25Cr side close to the weld metal has undergone a bainitic transformation. The increase in the hardness of 2.25Cr–1Mo side due to contact with liquid pool, consequent phase transformation leading to microhardness greater than 350 VHN has been studied [10] in earlier papers. Similar observations of microscopically distinct zones in weldments of ferritics have also been reported [11].

4.2. Formation of soft and hard zones

The exposure of the dissimilar weldments to elevated temperature of 1023 K has resulted in the following changes in the hardness profiles: (1) The overall hardness of the weldments has reduced to half the value of the 'as welded' condition, (2) the hardness of the base metal far away from the fusion line does not show significant change, between the shortest time of 1 h employed and the longest time of 15 h, (3) in all the weldments, exposed to 1023 K, a soft zone with hardness around (190–120 VHN) is seen near the 2.25Cr–1Mo side. Simultaneously a hard zone with hardness around 280 VHN is seen near the 9Cr weld region, and (4) the hardness of these zones vary with aging time and slows down considerably for longer aging times. Similar behaviour is seen for the width of these zones also. These features will now be discussed.

The overall reduction in the hardness of the weldment is due to the progress of the tempering process at 1023 K. The constancy of the hardness value between

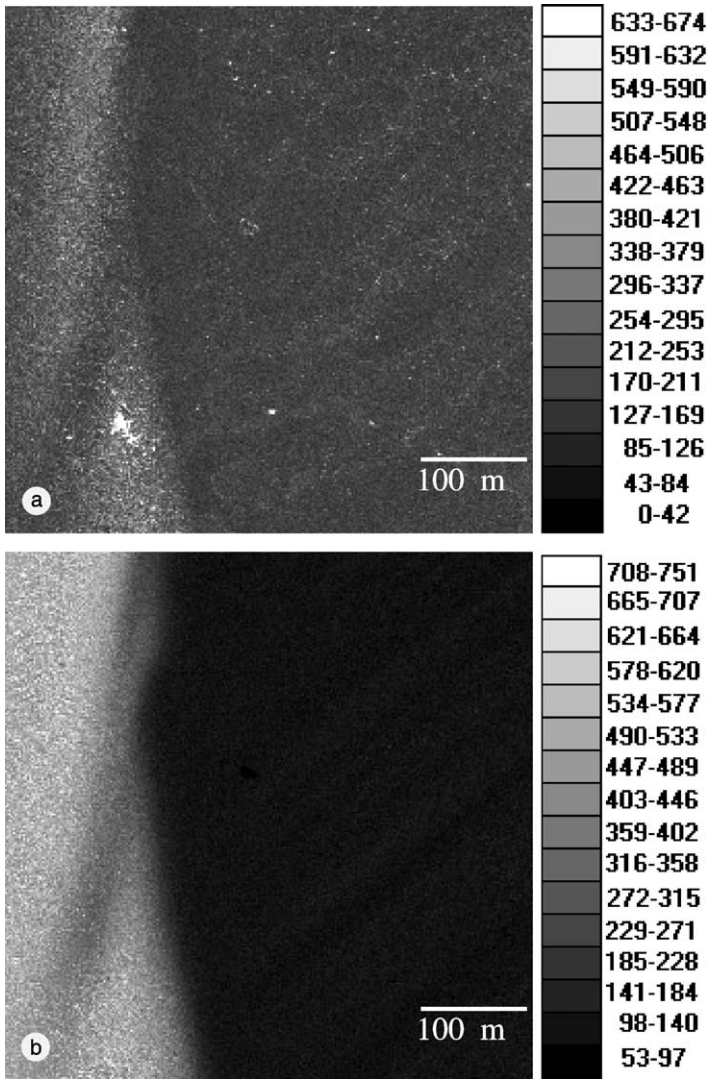

Fig. 10. X-ray image for (a) C, (b) Cr for 1023 K 15-h heat treated sample, taken from the interface between the weld metal and the 2.25Cr–1Mo base metal. The regions which are rich in Cr are found to be enriched in carbon also suggesting the formation of Cr rich carbides in hard zone.

the shortest time of 1 h and longer aging times, at distances far away from the fusion line is due to the fact that most of the tempering process is completed within the shortest aging time of one hour, at such high temperature of 1023 K.

The focus of the present study, namely, the formation of the soft and hard zones in the dissimilar weldments at high temperatures need to be discussed in the light of the associated microstructural and microchemical changes.

Confining the discussion to the origin of the formation of the soft zones first, the following observations are important: the hardness of the soft zone is as low as 200 VHN within an hour of exposure at 1023 K against the base metal hardness of 230 VHN for the same time of aging (Fig. 5(a)). The microstructure of the corresponding region (Fig. 4(a)) is distinct from that of the base metal. Fig. 3(d) clearly shows the presence of 'ferrite' grains in the soft zone on prolonged aging and Fig. 3(a) shows a 'bainite' (tempered) structure in the base metal. The above observations are consistently observed for all the aging times at 1023 K. The distinct reduction in the hardness of the regions near 2.25Cr–1Mo steel and the conversion of the bainitic structure of the base metal to ferrite structure, selectively in this zone, at all aging times suggest that this region has suffered 'depletion' of carbon, when exposed to 1023 K. The low

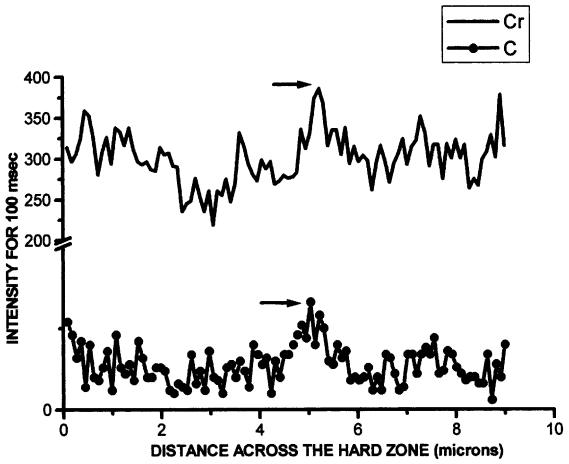

Fig. 11. Variation of X-ray intensity profile for chromium and carbon across the hard zone for 1023 K 15-h heat treated sample suggesting the formation of chromium rich carbides (the arrow marks indicate the simultaneous increase in both Cr and C intensities on the hard zone).

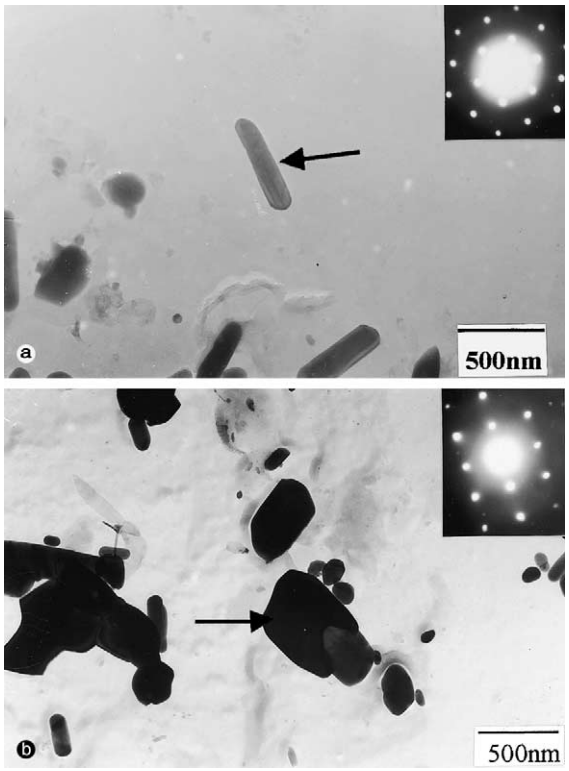

Fig. 12. Transmission electron micrographs and the respective SAD patterns from carbides in the hard zone of 2.25Cr–1Mo and 9Cr–1Mo weldment after exposure to 1023 K for 15 h. The SAD patterns in the insets are taken from carbides arrow marked in a and b respectively. Zone axes of the patterns are along $\langle 1\,1\,1\rangle$ in (a) and $\langle 2\,3\,3\rangle$ in (b).

concentration of carbon expected, made it impossible to provide direct confirmation of the depletion. The formation of soft zone can be explained in terms of the diffusion of carbon from low chrome to high chrome side. Difference in the activity of carbon between the base metal and the weld metal acts as the driving force for the diffusion of carbon. As a result of diffusion, the thermodynamic equilibrium is disturbed and to maintain the equilibrium, the carbides dissolve into the matrix converting the ferrite–bainite structure to ferrite.

A similar line of analysis for the origin of formation of hard zone near the 9Cr–1Mo weld metal side, suggest the following: the hardness of the hard zone is ~280 VHN against that of the weld metal of 270 VHN, within an hour of aging at 1023 K (Fig. 5(a)). As the time of heat treatment was increased, hardness of the hard zone showed marginal decrease from 280 to 265 VHN. However, the corresponding optical micrographs do not provide clear evidence for any microstructural changes. The dark etch regions suggest the formation of high density of fine precipitates, whose sizes are probably, below the resolution limit of the optical microscope. However, secondary electron image in Fig. 3(c) provide direct confirmation for the formation of precipitates in hard zone. The significant increase in Cr counts for the heat treated specimen (Fig. 7(a)) on the weld metal side may be due to the presence of Cr rich precipitates on the hard zone. In the as welded specimen Cr intensity is around 35 counts till a distance of about 0.1 mm after which it increases to around 60 counts. This indicates that the zone of the weld metal close to the interface has undergone dilution to a distance of 0.1 mm. The hardness value of this zone was found to be around 412 VHN which is close to that of the weld metal. Hence it can be said that despite a strong evidence for the formation of dilution zone, the experimental results do not provide confirmation for the modification of the microstructure and properties due to this zone. Observation of an increase in C counts in Fig. 7(b) on the weld metal side shows that the hard zone may consist of carbides. The difference in carbon counts observed between the as welded and the heat treated specimen on the weld metal side is due to the migration of carbon from the 2.25Cr base metal side to 9Cr weld metal side after PWHT. The scatter observed in Cr concentration on the weld metal side of the interface also suggests the presence of Cr rich precipitates on the hard zone. The simultaneous enrichment of Cr and C in the hard zone (Figs. 8 and 11) and the X-ray image (Fig. 10) suggest the formation of Cr rich carbides. SAD patterns obtained from the precipitates in hard zone confirmed that they are Cr rich $M_{23}C_6$ carbides. Different morphology of $M_{23}C_6$ in Fig. 12(a) and (b) suggests that the carbides might have been in different stages of growth. Determination of the exact amount of solutes present in the hard zone in EPMA is

futile since the contribution to the measured X-ray intensity from the matrix cannot be avoided. The relative differences in the carbon content, i.e. its enrichment in the hard zone as against its lower level is shown in Fig. 8(c) and (d). In the light of these evidences, it is possible to conclude that the hard zone represents the region rich in carbon.

The above evidences for the enrichment of carbon in the hard zone is due to enclosing a high density of fine carbides within the beam diameter during the EPMA analysis. Therefore, no attempt has been taken to convert the intensity values to absolute values of concentration of carbon in the ferrite matrix. A detailed analytical transmission electron microscopy work is in progress to arrive at this value. However, EPMA results could unambiguously show that the origin of the hard zone is due to the enrichment of carbon in this layer. Subsequently carbon must have precipitated into carbides. A similar unambiguous evidence for the depletion of carbon in the soft zone is impossible, since the carbon concentration that is to be analysed is very low, of the order of 0.1% and less. In such a situation, its manifestation in the microstructure namely conversion of bainite to ferrite, helped to deduce the depletion of carbon, confirmed by the corresponding enrichment in the adjacent layer.

Thus, it is clear that the formation of the soft and hard zones observed in the present study is due to the depletion and enrichment of carbon in the low Cr and high Cr side respectively. The depletion of carbon in the low Cr side stabilises ferrite, thus causing the observed change in the structure in the low chromium side. Grain growth could also be observed (Fig. 3(a)) in the soft zone due to the absence of pinning effect of carbides in the ferrite matrix. The enrichment of carbon in the adjacent layer results in the extensive precipitation of chromium carbides, as suggested by the SEM observations and simultaneous enhancement of chromium and carbon in the hard zone, which is confirmed by the electron diffraction evidences.

4.3. Variation in the width of the zones

Fig. 6(a) and (b) shows that the width of the zones and the hardness changes in the zones slow down significantly after certain aging times. While the width of the soft zone increases up to 320 μm (10 h) before slowing down, the hard zone grows up to only about 100 μm. Similarly, the hardness of the soft zone reduces from 190 to 130 VHN in about 5 h time, the change in the hard zone is only marginal. This type of behaviour also, indirectly, suggest a 'diffusion' related process to be the cause for the formation of the zones. Observation of the 'slowing down' of the changes in hardness and width in Fig. 6(a) and (b) also suggest the presence of opposing forces to the unrestricted growth of the zones.

4.4. Micromechanisms that take place during PWHT of dissimilar weldments

Based on the above discussions of the present results, it is possible to arrive at a comprehensive understanding of the different stages of the microscopic processes that may take place during PWHT of dissimilar weldments, which is described below: Fig. 13 shows the flow chart of the micromechanisms leading to the formation of soft and hard zones during exposure of dissimilar weldments to elevated temperature.

Stage 1: The normalised and tempered 2.25Cr–1Mo and 9Cr–1Mo steels, when welded together, suffer microstructural changes in regions close to the heat source.

Stage 2: On PWHT, carbon migrates out from the low Cr side to the high Cr side. Activity of carbon at the low chromium side is higher than in the higher chromium side according to the following equation:

$$a_C = N_C(\exp(N_A\varepsilon_C^A + N_B\varepsilon_C^B)),$$

where a_C is the activity of carbon, N_A, N_B and N_C are the number of A, B (constituent atoms) and carbon atoms present in the alloy. ε_C^A and ϵ_C^B represent the Wagner interaction parameters in ferrite. ε_C^{Cr} is negative for chromium, hence activity of carbon on 2.25Cr–1Mo side is greater than the 9Cr–1Mo side. At high temperatures, carbon diffusion takes place due to the driving force provided by this difference in the activity of carbon (only free carbon or carbon in solution of ferrite) at the two sides.

Stage 3: On PWHT, migration of carbon from the low Cr side to the high Cr side takes place disturbing the thermodynamic equilibrium on the low chrome side. To maintain the equilibrium, carbides dissolve into the matrix leading to the transformation of bainite in low Cr steel to ferrite. As a result, soft zone forms near the low Cr side of the dissimilar weldment.

Stage 4: Carbon, on arriving at high Cr side, reacts with chromium and forms chromium rich carbides, leading to the formation of hard zone.

Stage 5: Onset of slowing down in the width of zones could be due to constraints on the continued migration of carbon from the low Cr steel to high Cr steel. These could be due to the following reasons: (1) decrease in the difference in the activity of carbon between the two sides, caused by (a) depletion of chromium in the weld metal due to the formation of carbides, (b) rejection of C from the 2.25Cr base metal and (c) lower carbon level in the (transformed)

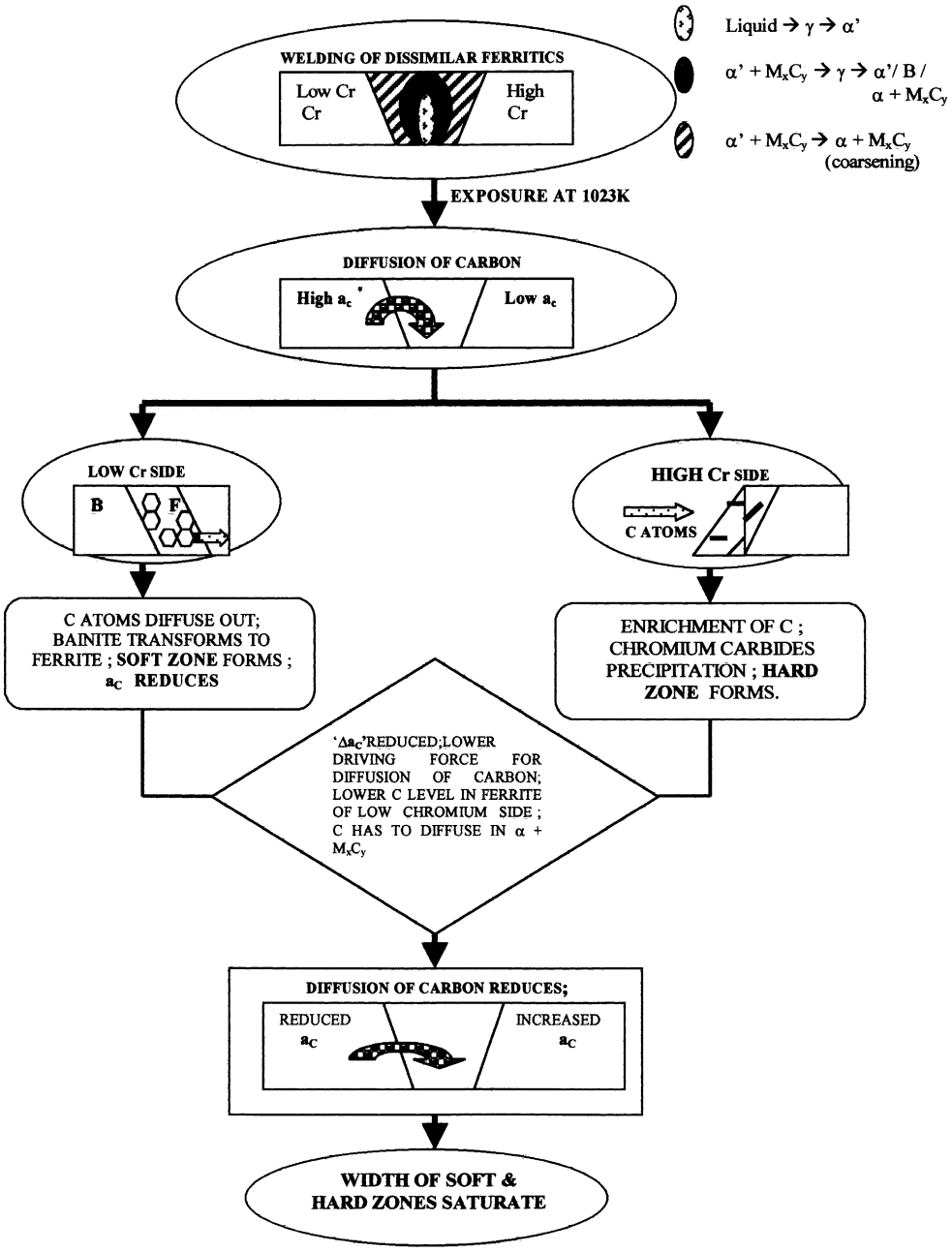

Fig. 13. Schematic representation of the micromechanisms operative during the formation of soft and hard zones in dissimilar weldments of ferritics, during high temperature exposure (a_C – activity of carbon, Δa_C – difference in the activity of carbon).

ferrite region of 2.25Cr base metal side and (2) formation of higher density of chromium rich carbides in the 'diffusion paths' of carbon atoms, inhibiting further diffusion of carbon atoms.

The restraining forces begin to restrict the migration of carbon leading to the observed slowing down in the width and hardness of zones. From the carbon activity diagram proposed by Chopra et al. [12], carbon activity in 2.25Cr–1Mo steel is found to be higher than that in 9Cr–1Mo steel. The negative interaction parameter of Cr, which is a ferrite stabilising element is known [6] to act as the driving force for the diffusion of carbon. Hence on PWHT, it is shown that carbon atoms migrate down the activity gradient from low Cr to high Cr side.

5. Conclusion

Following main conclusions can be drawn from the above studies:

1. Exposure of dissimilar weldments of 9Cr–1Mo and 2.25Cr–1Mo steels to elevated temperatures results in the formation of a carbide rich zone in the high chromium side and carbon depleted zone on the low chromium side of the weldment. Width and hardness of these zones are influenced by the duration of heat treatment. The change in the width and hardness of soft as well as hard zones slows down considerably after 15 h at 1023 K.
2. Carbon which diffuses to the high Cr side, gets precipitated in the form of chromium rich carbides leading to the 'precipitate rich' or hard zone on the weld metal side, characterised by a high hardness value.
3. A ferrite matrix characterised by a low hardness value called as the soft zone is formed on the HAZ region of 2.25Cr–1Mo base metal.
4. There is found to be no redistribution of molybdenum across the 9Cr–1Mo weld metal and 2.25Cr–1Mo base metal interface, whereas the qualitative as well as the quantitative analysis clearly shows the redistribution of carbon.
5. The micromechanisms operative at various stages of the growth of soft and hard zones are identified.

Acknowledgements

The authors have great pleasure in acknowledging the constant support and encouragement of Dr Baldev Raj, Director, Materials Chemistry and Reprocessing Group, IGCAR and Dr V.S. Raghunathan, Associate Director, Materials Characterisation Group, IGCAR. The authors wish to thank the perseverant efforts of Shri V. Thomas Paul to obtain the difficult TEM evidences for confirming the presence of carbides in the hard zone.

References

[1] S.K. Albert, T.P.S. Gill, A.K. Tyagi, S.L. Mannan, S.D. Kulkarni, P. Rodriguez, Welding J. 76 (3) (1997) 35s.
[2] B.C. Kim, H.S. Ann, J.T. Song, in: S.A. David, J.M. Vitek (Eds.), International trends in Welding Science and Technology, ASM International, Materials Park, OH, 1992, p. 307.
[3] J.M. Race, H.K.D.H. Bhadeshia, in: S.A. David, J.M. Vitek (Eds.), International trends in Welding Science and Technology, ASM International, Materials Park, OH, 1992, p. 315.
[4] C.D. Lundin, K.K. Khan, D. Yang, Report No. 1, WRC Bulletin 407 (1996) 1.
[5] C.D. Lundin, K.K. Khan, D. Yang, in: S.A. David, J.M. Vitek (Eds.), Recent trends in Welding Science and Technology, ASM International, Materials Park, OH, 1990, p. 291.
[6] B. Bachmayr, H. Cerjak, M. Witwer, J.S. Kirkaldy, in: S.A. David, J.M. Vitek (Eds.), Recent trends in Welding Science and Technology, ASM International, Materials Park, OH, 1990, p. 237.
[7] N.F. Eaton, B.A. Glossop, Metal Construct. Brit. Weld. J. 1 (12) (1969) 6.
[8] C.D. Lundin, in: S.A. David (Ed.), Advances in Welding Science and Technology, ASM International, Materials Park, OH, 1986, p. 475.
[9] S.K. Albert, G. Srinivasan, T.P.S. Gill, in: Proc. of National Welding Seminar, The Indian Institute of Welding, Bangalore, 1997, p. 222.
[10] P. Parameswaran, V. Thomas Paul, M. Vijayalakshmi, V.S. Raghunathan, in: Presented at Annual Technical Meeting of Indian Institute of Metal, Jamshedpur, India, 1997.
[11] M. Vijayalakshmi, S. Saroja, V. Thomas Paul, R. Mythili, V.S. Raghunathan, Metall. Mater. Trans. 30A (1999) 161.
[12] O.K. Chopra, K. Natesan, T.F. Kassener, J. Nucl. Mater. 96 (1981) 269.